

The wake of a two-dimensional ship in the low-speed limit: results for multi-cornered hulls

Philippe H. Trinh[†] and S. Jonathan Chapman

Oxford Centre for Industrial and Applied Mathematics, Mathematical Institute, 24-29 St. Giles', Oxford,
Oxfordshire OX1 3LB, UK

(Received 22 August 2012; revised 13 October 2013; accepted 1 November 2013)

In the Dagan & Tulin (*J. Fluid Mech.*, vol. 51, 1972, pp. 529–543) model of ship waves, a blunt ship moving at low speeds can be modelled as a two-dimensional semi-infinite body. A central question for these reduced models is whether a particular ship design can minimize, or indeed eliminate, the wave resistance. In the previous part of our work (Trinh *et al.*, *J. Fluid Mech.*, vol. 685, 2011, pp. 413–439), we demonstrated why a single corner can never be made waveless. In this accompanying paper, we continue our investigations with the study of more general piecewise-linear, or multi-cornered ships. By using exponential asymptotics, we demonstrate how the production of waves can be directly ascertained by the positions and angles of the corners. In particular, this theory answers the question raised by Farrow & Tuck (*J. Austral. Math. Soc. B*, vol. 36, 1995, pp. 424–437) as to why certain bulbous-like obstructions can minimize the production of waves. General results for wavelessness are given for a class of hulls, and numerical computations of the nonlinear ship-wave problem are used to confirm analytical predictions. Finally, we discuss open questions regarding hulls without corners and more general three-dimensional bluff bodies.

Key words: surface gravity waves, wave–structure interactions, waves/free-surface flows

1. Introduction

The investigations in this paper are focused on the analysis of the low-speed or low-Froude-number wave models proposed by Dagan & Tulin (1969, 1972), in which blunt-bodied ships are studied in the context of potential flow and asymptotic expansions in powers of the Froude number (the Froude number represents the ratio between inertial and gravitational forces). As a particularly interesting case that draws our attention, we recall the work of Farrow & Tuck (1995), who showed that by attaching a bulbous-like obstruction to an otherwise rectangular ship's stern, one could produce a dramatic effect on the production of transverse waves. As they reported in their paper:

At this [Froude number], a rectangular stern generates waves with steepness 0.0855, whereas the stern with the downward-pointing bulb [...] yields waves with steepness 0.0119. It is clear that the addition of the downward-pointing bulb has had a dramatic effect on the downstream wave steepness, reducing it by a factor of 7.2, although it has still not eliminated the waves entirely.

[†] Email address for correspondence: trinh@maths.ox.ac.uk

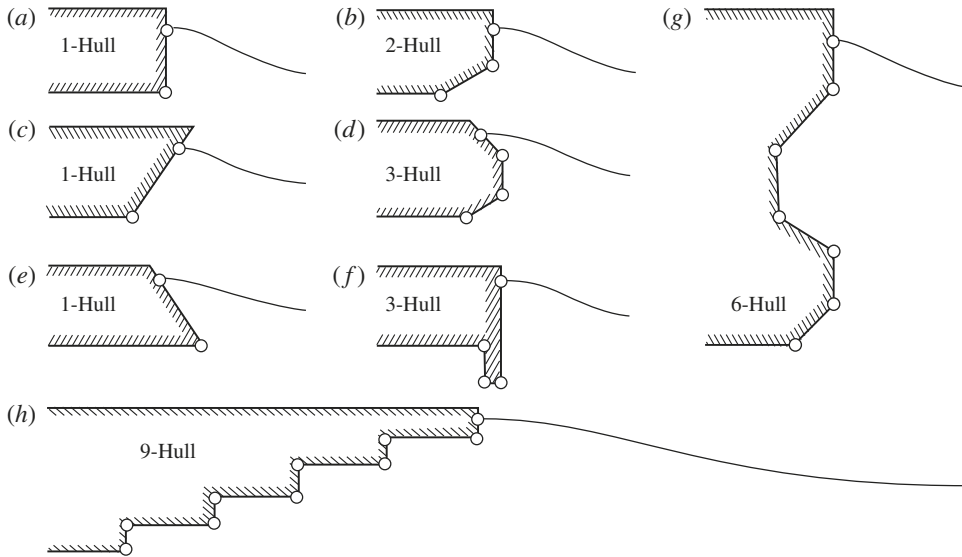


FIGURE 1. Are any of these ships waveless? In all cases, the flow is from left to right and nodes indicate singularities in the analytic continuation.

Our goal is to give an analytical criterion that explains why this phenomenon occurs; that is to say, what distinguishes the two ships, one with a bulb and one without a bulb, in the context of the ‘slow-ship’ approximation? The advantage of the slow-ship potential-flow approximation is that it allows us to directly relate the generation of waves to the shape of the ship’s hull without the need for numerical simulations.

In addition to addressing the Farrow & Tuck (1995) issue, we are also interested in a more general question: in the low-speed limit, when a blunt ship is modelled as a two-dimensional semi-infinite body, can it ever be made waveless? These waveless or wave-minimization questions in the context of the Dagan & Tulin (1972) approximation were studied by Vanden-Broeck & Tuck (1977), Vanden-Broeck, Schwartz & Tuck (1978), Madurasinghe & Tuck (1986), and Tuck (1991*a,b*) for ship hulls of varying geometries, and we are interested in continuing their line of inquiry.

In the previous part of our work (Trinh, Chapman & Vanden-Broeck 2011), we demonstrated that piecewise-linear hulls with a single, submerged corner can never be made waveless; thus consequently, a free surface that attaches to a single-cornered bow at a stagnation point is not possible within the Dagan & Tulin (1972) model. For the case of piecewise-linear hulls with multiple corners, the answer to this question is not as clear. For example, are any of the eight hulls presented in figure 1 waveless? If not, then which ones produce the smallest waves? For the case of potential flow over a submerged obstruction, waveless configurations are certainly possible, as was demonstrated by Lustri, McCue & Binder (2012) and Hocking, Holmes & Forbes (2012), but the same question for surface-piercing ships of general form remains open. Certainly, there are notable difficulties in studying this problem. For example, waveless ships were proposed by Tuck & Vanden-Broeck (1984) and Madurasinghe & Tuck (1986), but these were later refuted in the more comprehensive numerical study by Farrow & Tuck (1995), in which they showed that

The free surface would at first sight appear to be waveless, but on closer examination of the numerical data, there are very small waves present and they have a steepness of 1.5×10^{-3}

in reference to the bulbous hull in Tuck & Vanden-Broeck (1984). Our desire, then, is to study these issues in terms of the low-Froude-number asymptotic expansions.

Having progressed through the theory of Trinh *et al.* (2011), we know that at low Froude numbers, the waves generated by a ship become exponentially small and are thus invisible to a regular asymptotic expansion. The ineffectiveness of traditional asymptotics in capturing the low-speed limit was first noted by Ogilvie (1968, 1970) and later termed the *low-speed paradox*. Techniques in exponential asymptotics (Boyd 1998) allow us to demonstrate the fact that these hidden waves are switched-on when the regular expansion is continued across critical curves (*Stokes lines*) in the complex plane; this process is known as the *Stokes phenomenon*. Most important, however, is the valuable insight that these approximations give: an explicit formula that relates the shape of an arbitrary hull with its resultant waves. The question of wavelessness in the low-Froude-number limit is then simplified to examining whether the sum of the Stokes-line contributions can ever be zero in regions far from the ship.

The requisite background in exponential asymptotics can be found in Trinh *et al.* (2011). The techniques we apply are based on the use of a factorial-over-power ansatz to capture the divergence of the asymptotic expansions, then optimal truncation and Stokes-line smoothing to relate the late-order terms to the exponentially small waves (see for example, papers by Olde Daalhuis *et al.* 1995, Chapman, King & Adams 1998, and Trinh 2010a). Our paper also parallels the works of Chapman & Vanden-Broeck (2002, 2006) and Trinh & Chapman (2013a,b) on the application of exponential asymptotics to the study of gravity or capillary waves produced by flow over a submerged object.

1.1. *The role of low-Froude-number approximations and an outline of the paper*

It is important for us to mention that the low-Froude-number model of Dagan & Tulin (1972) is indeed a very idealized approximation for understanding the production of ship waves. Real stern and bow flows are very complex, and viscosity, turbulence, and necklace vortices can all play an important role in the production of waves. We refer the reader to, for example, some of the numerical simulations of Grosenbaugh & Yeung (1989) and Yeung & Ananthakrishnan (1997) that demonstrate some of the complex dynamics that arise in ship flows once, for example, vorticity and viscosity are included. In § 6 of this paper, we shall return to discuss the caveats of the low-speed approximation.

Ultimately, we are interested in obtaining analytical intuition about the connection between the ship's hull and the waves produced. The more usual routes towards analytical solutions assume an asymptotically small geometry, which leads to the 'thin-ship', 'flat-ship' or 'streamline-ship' approximations; in such regimes, a waveless ship is impossible (see for example, Kotik & Newman 1964 and Krein in Kostyukov 1968), but these theories say very little about the case of non-thin ships. Other examples of ship-wave models can be studied, including the Kelvin–Neumann formulation in which the free-surface condition is linearized about a steady uniform stream and the boundary condition on the ship's hull is satisfied exactly, but generally these problems do require a degree of numerical computation. A discussion of such problems can be found in the book by Kuznetsov, Maz'ya & Vainberg (2002) and the review and discussion by Newman *et al.* (1991) (see e.g. Pagani & Pierotti 2004

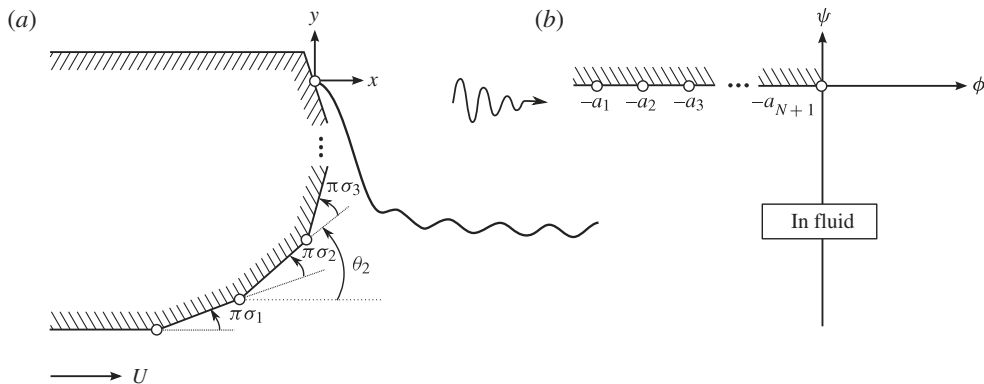


FIGURE 2. Flow past a piecewise-linear N -hull. The N corners of exterior angles $\pi\sigma_1, \pi\sigma_2, \dots, \pi\sigma_N$ in the (x, y) plane (a) are mapped to $w = -a_1, -a_2, \dots, -a_N$ in the complex potential plane (b). The stagnation point is $w = -a_{N+1} = 0$.

for more recent work on rigorous results applicable to non-slender geometries). We finally refer readers to the reviews by Tuck (1991a) and Tulin (2005) for a summary of the role played by low-Froude-number approximations, particularly in connection with problems in which we require asymptotic solutions that preserve the nonlinearity of the geometry.

The paper will proceed as follows. First, the mathematical formulation of the ship-wave problem is briefly recapitulated in § 2. This is followed by the asymptotic analysis of the low-Froude-number problem in § 3, which culminates in the derivation of explicit expressions for the wake of an arbitrary multi-cornered ship. From these analytical results, we explain why certain classes of multi-cornered ships can never be made waveless in § 4, then in § 5, these theoretical results are vindicated by comparisons with numerical computations.

2. Mathematical formulation

Consider steady, incompressible, irrotational, inviscid flow in the presence of gravity, past the semi-infinite body shown in figure 2, which consists of a flat bottom and a piecewise-linear front face. With tildes denoting dimensional quantities, we assume that there is a uniform stream of speed U as $\tilde{x} \rightarrow -\infty$, and that the flow attaches to the stern at a stagnation point, $\tilde{x} = 0$ and $\tilde{y} = 0$. We note that in the context of potential flow, any free-surface profile corresponding to stern flow, with $U > 0$, can be applied to bow flow, with $U < 0$, as long as the radiation conditions are satisfied (cf. Stoker 1957, p. 174). In the context of gravity waves and for the situation shown in figure 2, a solution for bow flow would require the free surface to be flat as $\tilde{x} \rightarrow \infty$.

We shall refer to a piecewise-linear hull with N corners as an ‘ N -hull’. Introducing the dimensional velocity potential by $\tilde{\phi} = \nabla\tilde{u}$, we choose the zero level for the potential such that $\tilde{\phi} = 0$ at the stagnation point. An N -hull will be specified by N points along the negative real axis,

$$\tilde{\phi} = -\tilde{a}_k \quad \text{with} \quad -\tilde{a}_1 < -\tilde{a}_2 < \dots < -\tilde{a}_n, \quad k = 1, 2, \dots, N \quad (2.1)$$

representing the corners in the potential plane, and with $\tilde{\phi} > 0$ corresponding to the free surface. Along with the positions of the corners, the geometry of the hull can be

described by specifying the angle, θ , of the hull with respect to the \tilde{x} -axis along each of the $k = 1, 2, \dots, N$ linear segments of the solid boundary, $\phi < 0$. We write

$$\theta(\tilde{\phi}) = \theta_k = \pi \sum_{j=1}^k \sigma_j \quad \text{for } \tilde{\phi} \in (-\tilde{a}_k, -\tilde{a}_{k+1}), \quad (2.2)$$

where $\pi\sigma_k$ is the exterior angle at the k th corner (see figure 2) and we set $\tilde{a}_{N+1} = 0$ for the stagnation point. When $N = 2$, we will occasionally refer to the two-cornered ship as a $[\sigma_1, \sigma_2]$ -hull.

The dimensional problem can now be re-posed in terms of a non-dimensional boundary-integral formulation. The derivation for one-cornered ships is found in Trinh *et al.* (2011) and the one notable difference is that here we prefer to choose

$$L = \frac{K}{U}, \quad \text{where } K = \sum_{i=1}^N |\tilde{\phi}(-\tilde{a}_i)|, \quad (2.3)$$

as the characteristic length scale. In the one-cornered problem, $-K$ is the value of the potential at the single corner. To non-dimensionalize, we set

$$\tilde{x} = Lx, \quad \tilde{y} = Ly, \quad u = U\tilde{u}, \quad \tilde{\phi} = K\phi. \quad (2.4)$$

We now seek the non-dimensional governing equations within the complex potential (ϕ, ψ) -plane, where the streamfunction, ψ , is the harmonic conjugate of ϕ and $\psi \leq 0$ within the fluid. The unknowns are the fluid speed $q = q(\phi, \psi)$, and streamline angles, $\theta = \theta(\phi, \psi)$, measured from the positive x -axis, which satisfy the combination

$$q e^{-i\theta} = u - iv \quad (2.5)$$

for horizontal and vertical velocities, u and v . The body and free surface are given by the streamline $\psi = 0$, with $\phi < 0$ for the body and $\phi > 0$ for the free surface.

The free surface is then obtained by solving a boundary-integral equation, coupled with Bernoulli's condition:

$$\log q = \frac{1}{\pi} \int_{-\infty}^{\infty} \frac{\theta(\varphi)}{\varphi - \phi} d\varphi, \quad (2.6a)$$

$$\epsilon q^2 \frac{dq}{d\phi} = -\sin \theta, \quad (2.6b)$$

on $\psi = 0$, and where we have introduced the non-dimensional parameter

$$\epsilon = \frac{U^3}{gK}, \quad (2.7)$$

which is related to the square of the Froude draft number. The N corners are specified by points $\phi = -a_k$ for $k = 1, 2, \dots, N$ and because of the choice of scaling (2.3), the positions of the corners satisfy the normalization property

$$\sum_{k=1}^{N+1} a_k = 1 \quad \text{with } a_{N+1} = 0. \quad (2.8)$$

2.1. Complexification of the free surface

Using the hull angles from (2.2) in (2.6a), we write the portion of the boundary integral over the negative real axis as

$$\frac{1}{\pi} \int_{-\infty}^0 \frac{\theta(\varphi)}{\varphi - \phi} d\varphi = \log \left[\prod_{k=1}^{N+1} (\phi + a_k)^{-\sigma_k} \right] \equiv \log q_s(\phi), \quad (2.9)$$

where the power, σ_{N+1} , in the product is defined according to the requirement that the free surface approaches the uniform stream, with $\theta \rightarrow 0$ and $q_s \rightarrow 1$ as $\phi \rightarrow \infty$. From (2.9), this gives

$$\sigma_{N+1} = - \sum_{j=1}^N \sigma_j. \quad (2.10)$$

The function q_s in (2.9) serves to distinguish the geometry of different piecewise-linear ships. Note also that the product representation of the complex quantity q_s can be alternatively derived by using a Schwartz–Christoffel mapping applied to the polygonal hull shape and a rigid, flat free surface (also known as the rigid-wall solution).

With particular choices for the corner positions, $\phi = -a_k$, and corner angles, σ_k , the free-surface velocity $qe^{-i\theta}$ can be numerically computed using (2.6) and (2.9). However, as explained in Trinh *et al.* (2011, §3), the exponentially small free-surface waves in the low-Froude-number limit, $\epsilon \rightarrow 0$, arise due to the Stokes phenomenon. To study this, we must analytically continue the free surface $\psi = 0$. Since the free surface is parametrized by ϕ , this means that we allow ϕ to take on complex values. Similarly, the velocity $q(\phi, 0)$, and streamline angle $\theta(\phi, 0)$ are analytically continued, so that these, too, will be complex-valued for complex ϕ .

There is a useful correspondence here between the complexified free surface and the fluid region, which we now endeavour to explain. The complex velocity,

$$\mathcal{U}(w) = qe^{-i\theta}, \quad (2.11)$$

is an analytic function of the complex potential $w = \phi + i\psi$. On the free surface, $\psi = 0$, the complex velocity is therefore equal to $\mathcal{U}(\phi)$, which we will label $\mathcal{U}_s(\phi)$. Now when we analytically continue the free surface by allowing ϕ to take on complex values, the value of the analytically continued \mathcal{U}_s at the point $\phi = \phi_r + i\phi_i$ ($\phi_r, \phi_i \in \mathbb{R}$) is simply the value of \mathcal{U} at the point $w = \phi_r + i\phi_i$, i.e. at $\phi = \phi_r$, $\psi = \phi_i$. Thus each point in the complexified free surface can be identified with a point in the real physical fluid or possibly its continuation (since real fluid only exists for $\psi < 0$, but the complexified free surface exists for all values of ϕ_i).

It is due to this correspondence between the complexified free surface and real physical fluid that, within the context of low-Froude-number free-surface flows, we often refer to a physical property (e.g. the corner of a ship) as generating a Stokes line. Note also that this correspondence only holds for analytic functions of w . Although the combination $qe^{-i\theta}$ takes the same values at the point $\phi = \phi_r + i\phi_i$, $\psi = 0$ (on the complexified free surface), and the point $\phi = \phi_r$, $\psi = \phi_i$ (in the fluid), the same is not true of the individual functions q and θ .

To emphasize this correspondence, and the fact that ϕ is complex, we relabel ϕ as w in the analytically continued equations. Then analytically continuing (2.6a) and (2.6b)

gives

$$\log q \pm i\theta = \log q_s(w) + \mathcal{H}\theta(w), \quad (2.12a)$$

$$\epsilon q^2 \frac{dq}{dw} = -\sin \theta, \quad (2.12b)$$

where the \pm signs correspond to analytic continuation into the upper and lower half- ϕ -planes, respectively, and \mathcal{H} denotes the Hilbert transform operator on the free surface,

$$\mathcal{H}\theta(w) = \frac{1}{\pi} \int_0^\infty \frac{\theta(\varphi)}{\varphi - w} d\varphi. \quad (2.13)$$

The remainder of this paper will be devoted to studying the two equations in (2.12).

3. Exponential asymptotics

A single-cornered ship will always produce exponentially small waves in the low-Froude-number limit, $\epsilon \rightarrow 0$; these waves are explained by the presence of a Stokes line which emerges from the singularity at the corner. For a multi-cornered ship, the analysis proceeds almost identically to Trinh *et al.* (2011), except now each corner of the hull has the potential to produce Stokes lines and its own separate wave contribution. In this section, we shall briefly re-apply the methodology of the previous work, and provide the corresponding formulae for the case of an N -hull.

3.1. Late-order terms

Here, we perform the asymptotic analysis which corresponds to analytically continuing the free surface into the upper half- ϕ -plane; continuation into the lower half-plane produces a complex-conjugate contribution, which we add to our results, later.

We begin by substituting the usual asymptotic expansions

$$\theta = \sum_{n=0}^{\infty} \epsilon^n \theta_n \quad \text{and} \quad q = \sum_{n=0}^{\infty} \epsilon^n q_n, \quad (3.1)$$

into (2.12a) and (2.12b) (with the $+$ sign). In the limit $\epsilon \rightarrow 0$, the leading-order solution is the rigid-wall flow of (2.9),

$$\theta_0 = 0, \quad (3.2a)$$

$$q_0 = q_s = \prod_{j=1}^{N+1} (w + a_j)^{-\sigma_j}, \quad (3.2b)$$

while the $O(\epsilon)$ terms are

$$\theta_1 = -q_0^2 \frac{dq_0}{dw}, \quad (3.3a)$$

$$q_1 = iq_0^3 \frac{dq_0}{dw} + q_0 \mathcal{H}\theta_1(w). \quad (3.3b)$$

The key observation is that the leading-order solution, q_0 in (3.2b), possesses a singularity at each of the corners, $w = -a_k$. Since the solution at each subsequent order involves a derivative of the previous order, we would thus expect that as $n \rightarrow \infty$, the power of the singularity grows. At the late orders, the asymptotic expansions (3.1)

exhibit factorial-over-power divergence,

$$\theta_n \sim \sum_{k=1}^{N+1} \frac{\Theta_k \Gamma(n + \gamma_k)}{\chi_k^{n+\gamma_k}} \quad \text{and} \quad q_n \sim \sum_{k=1}^{N+1} \frac{Q_k \Gamma(n + \gamma_k)}{\chi_k^{n+\gamma_k}}, \quad (3.4)$$

where γ_k is complex constant, Q_k and χ_k are functions of the complex potential w . There is a *singular* χ_k (a term from Dingle 1973, p. 148), with $\chi_k(-a_k) = 0$, for each singularity of the leading-order problem (3.2b). For much of the analysis, we can simply choose one of the corners of interest and add the individual contributions at the end.

The singularities, $w = -a_k$, are located off the free surface, where the Hilbert transform in (2.12a) is evaluated and so, as justified in Trinh *et al.* (2011), $\mathcal{H}\theta_n(w)$ is exponentially subdominant to the terms on the left-hand side for large n . At $O(\epsilon^n)$, (2.12a) gives

$$\theta_n \sim i \frac{q_n}{q_0} - \frac{i q_1 q_{n-1}}{q_0^2} + \dots \quad (3.5)$$

as $n \rightarrow \infty$, and substitution into (2.12b) gives the relevant terms at $O(\epsilon^n)$:

$$[q_0^3 q'_{n-1} + i q_n] + \left[2q_0^2 q'_0 q_{n-1} + 2q_0^2 q_1 q'_{n-2} - i \frac{q_{n-1} q_1}{q_0} \right] + \dots = 0. \quad (3.6)$$

We substitute the ansatzes of (3.4) into (3.6), and this yields, at leading order as $n \rightarrow \infty$,

$$\frac{d\chi_k}{dw} = \frac{i}{q_0^3}. \quad (3.7)$$

Since χ_k is zero at each of the singularities, $w = -a_k$, we integrate (3.7) to give

$$\chi_k(w) = \int_{-a_k}^w \frac{i}{q_0^3(\varphi)} d\varphi. \quad (3.8)$$

At the next order in (3.6) and using the substitution (3.5) as $n \rightarrow \infty$, we find that

$$Q_k(w) = \frac{\Lambda_k}{q_0^2} \exp \left[3i \int_{w^\star}^w \frac{q_1(\varphi)}{q_0^4(\varphi)} d\varphi \right], \quad (3.9)$$

where Λ_k is constant, and w^\star is any point for which the integral is defined. Finally, (3.5) allows us to relate the two prefactors using $\Theta_k \sim iQ_k/q_0$, so that

$$\Theta_k(w) = \frac{\Lambda_k i}{q_0^3} \exp \left[3i \int_{w^\star}^w \frac{q_1(\varphi)}{q_0^4(\varphi)} d\varphi \right]. \quad (3.10)$$

With χ_k , Q_k , and Θ_k now determined, we have thus derived the late-orders behaviour in (3.4), subject to the values of γ_k and Λ_k ; these must be determined by applying the method of matched asymptotics near the singularity $w = -a_k$.

3.2. Stokes lines

From Trinh *et al.* (2011), we know that the components of the late-order terms (3.4) play a crucial role in determining the free-surface waves. Using the expression of χ_k in (3.8), Stokes lines can be traced from each of the ship's corners, across which the Stokes phenomenon necessitates the switching-on of waves. From Dingle (1973), these

special lines are given by the points $w \in \mathbb{C}$ where

$$\text{Im}[\chi_k(w)] = 0 \quad \text{and} \quad \text{Re}[\chi_k(w)] \geq 0. \tag{3.11}$$

We now examine the direction in which the Stokes line first emerges from its corresponding singularity. As $w \rightarrow -a_k$, we use (3.2b) to write

$$q_0 \sim c_k(w + a_k)^{-\sigma_k} \quad \text{where} \quad c_k = \prod_{\substack{j=1 \\ j \neq k}}^{N+1} (a_j - a_k)^{-\sigma_j}. \tag{3.12}$$

Substituting this into (3.8) yields

$$\chi_k \sim \left[\frac{i}{c_k^3(1 + 3\sigma_k)} \right] (w + a_k)^{1+3\sigma_k} \tag{3.13}$$

in the limit $w \rightarrow -a_k$. The condition that $\chi_k(-a_k) = 0$ requires that $\sigma_k > -1/3$. In other words, for there to be a singularity, the local deviation of the corner must be greater than $-\pi/3$. This is a necessary (but not sufficient) condition for there to be a free-surface wave produced by the corner. In fact, a stronger condition for the existence of a Stokes line emerging on the relevant Riemann sheet can be derived. We can write

$$\arg(c_k) = \sum_{j=k+1}^{N+1} \arg(a_j - a_k)^{-\sigma_j} = -\pi \sum_{j=k+1}^{N+1} \sigma_j = \theta_k, \tag{3.14}$$

where the last equality follows from applying (2.2) and (2.10), and applies for analytic continuation into the upper half-plane. Alternatively, (3.14) can be derived by noting that the complex velocity $q_0 e^{-i\theta_0} \sim u - iv$, and $\theta_0 = 0$, so the argument of c_k must correspond to the direction of the flow, θ_k , moving along the hull.

According to (3.11), we should search for directions in which $\arg(\chi_k) = 2m\pi$ for $m \in \mathbb{Z}$. If we write $\arg(w + a_k) = \nu_k$, then using (3.14) in (3.13), we see that Stokes lines must leave at angles of

$$\nu_k = \left(\frac{3\theta_k + 2m\pi - \pi/2}{1 + 3\sigma_k} \right), \tag{3.15}$$

where we need $\nu_k \in (0, \pi)$ in order for the line to emerge in the upper half-plane. The general requirements for a Stokes line to intersect the free surface would depend on the global properties of the leading-order flow, q_0 , but for most hulls, the requirement that $\nu_k \in (0, \pi)$ with (3.15) is adequate. With this in mind, let

$$\mathcal{J} \subseteq \{1, 2, \dots, N + 1\} \tag{3.16}$$

denote those corners, $w = -a_k$, $k \in \mathcal{J}$, that have a Stokes line crossing the free surface.

As an example, consider figure 3, which illustrates the Stokes lines for various N -hulls, including a simple 2-hull, the 3-hull of Farrow & Tuck (1995), a bulbous 6-hull, and a step-like 9-hull. With the exception of a single configuration, the condition that a Stokes line emerges into the upper half-plane is enough to guarantee that it intersects the free surface. The exception is with the 3-hull, for which the second singularity has a Stokes line emerging at an angle of $\nu_2 = 3\pi/5$, but which does not later encounter the free surface.

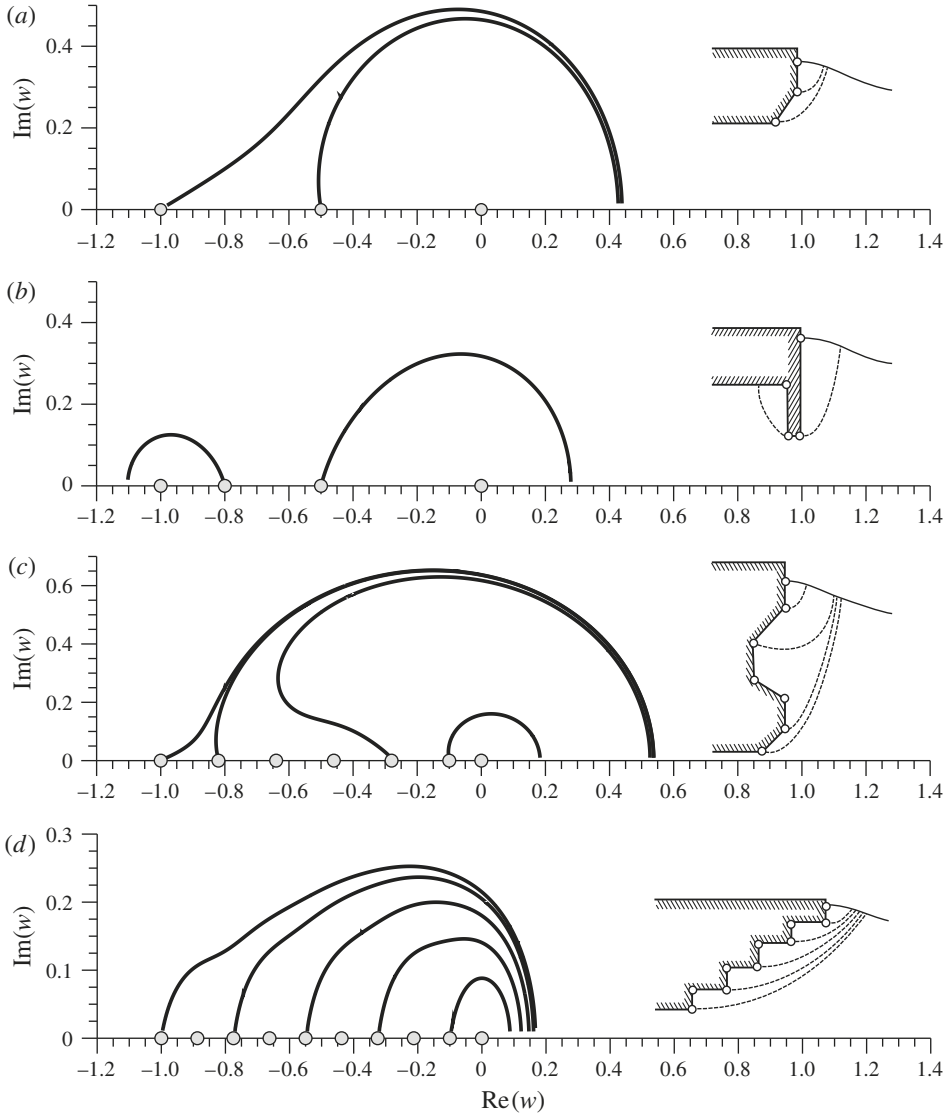


FIGURE 3. Stokes lines for (a) the 2-hull, (b) Farrow & Tuck’s (1995) 3-hull, (c) the 6-hull shown before in figure 2, and (d) the 9-hull. For the 2-hull and 6-hull, the corner angles diverge at $\pm\pi/4$; for the remaining hulls, the corner angles are all rectangular.

3.3. Stokes phenomenon and wave expression

The derivation of the exponentials that appear whenever a Stokes line is crossed (the Stokes phenomenon) follows the process outlined in Trinh *et al.* (2011) and Chapman & Vanden-Broeck (2006): we optimally truncate the asymptotic expansions (3.1) at $n = \mathcal{N}$, and examine the remainders. We then set

$$q = \sum_{n=0}^{\mathcal{N}-1} \epsilon^n q_n + S_{\mathcal{N}}, \tag{3.17}$$

with a similar expression for the series for θ . When \mathcal{N} is chosen to be the optimal truncation point, the remainder $S_{\mathcal{N}}$ is found to be exponentially small. By re-scaling near the Stokes line, it can be shown that a wave of the following form switches on:

$$\sim \frac{2\pi i}{\epsilon^{\gamma_k}} Q_k \exp \left[-\frac{\chi_k}{\epsilon} \right]. \tag{3.18}$$

To (3.18), we must also add the complex conjugate due to the contributions from analytic continuation of the free surface into the lower half- ϕ -plane (see (2.12a)). The sum of the two contributions is then

$$q_{exp,k} \sim \frac{4\pi}{\epsilon^{\gamma_k}} \operatorname{Re} \left\{ i Q_k \exp \left[-\frac{\chi_k}{\epsilon} \right] \right\}, \tag{3.19}$$

with one such expression for every relevant Stokes line, $k \in \mathcal{J}$.

Thus, for any given arbitrary N -hull with a geometry such that \mathcal{J} is non-empty, the appearance of exponentially small waves is a necessary consequence of the divergent low-Froude-number problem; in order to check that such a ship can never be waveless, we need to verify that the sum of all the contributions incurred can never be zero, so that there is a non-zero wave amplitude far downstream.

3.4. Wave formulae for N -hulls

The constants γ_k and Λ_k , which appear in the final form of the waves (3.19) (the latter as a prefactor in Q_k in (3.9)), can be determined by re-scaling w and q near each of the singularities, and then matching the leading-order nonlinear (inner) solutions with the late-order (outer) terms of (3.4). It can be shown (see (6.8) in Trinh *et al.* 2011) that

$$\gamma_k = \frac{6\sigma_k}{1 + 3\sigma_k} \tag{3.20}$$

and

$$\Lambda_k = \frac{c_k^{6-3\gamma_k} e^{i\pi\gamma_k/2}}{2C_k (1 + 3\sigma_k)^{\gamma_k}} \left[\lim_{n \rightarrow \infty} \frac{\phi_{n,k}}{\Gamma(n + \gamma_k)} \right], \tag{3.21}$$

where C_k is given by

$$C_k = q_0^3(w^\star) \exp \left(3i \int_{w^\star}^{-a_k} \frac{\mathcal{H}\theta_1(\varphi)}{q_0^3(\varphi)} d\varphi \right). \tag{3.22}$$

The terms $\phi_{n,k}$ are given by the recurrence relation,

$$\phi_{0,k} = 1, \tag{3.23}$$

$$\phi_{n,k} = \sum_{m=0}^{n-1} \left(m + \frac{2\sigma_k}{1 + 3\sigma_k} \right) \phi_m \phi_{n-m-1} \quad \text{for } n \geq 1. \tag{3.24}$$

We will often make reference to the limiting ratio in (3.21), so we define the function:

$$\Omega(\sigma_k) \equiv \lim_{n \rightarrow \infty} \frac{\phi_{n,k}}{\Gamma(n + \gamma_k)}. \tag{3.25}$$

The value of $\Omega(\sigma_k)$ only depends on the local divergence of the k th corner, and its values are given in Trinh *et al.* (2011). Since $\Omega \neq 0$ for all choices of the local

angle σ_k , Λ_k is also non-zero and this verifies that each of the $|\mathcal{J}|$ corners of an N -hull must necessarily generate a non-zero wave on the free surface.

With Q_k given by (3.9), Λ_k given by (3.21) and (3.25), and $\arg(c_k)$ from (3.14), we have from (3.19) the result that

$$q_{exp,k} \sim \frac{4\pi}{\epsilon^{\gamma_k}} \frac{|c_k|^{6-3\gamma_k}}{2(1+3\sigma_k)^{\gamma_k}} \frac{\Omega(\sigma_k)}{q_0^5} \exp \left[-\text{Im} \left(3 \int_{-a_k}^w \frac{\mathcal{H}\theta_1}{q_0^3} d\phi \right) \right] \exp \left[-\frac{\text{Re}(\chi_k)}{\epsilon} \right] \\ \times \cos \left[-\frac{\text{Im}(\chi_k)}{\epsilon} + \frac{\pi}{2} + \frac{\pi\gamma_k}{2} + (6-3\gamma_k)\theta_k + \text{Re} \left(3 \int_{-a_k}^w \frac{\mathcal{H}\theta_1}{q_0^3} d\phi \right) \right]. \quad (3.26)$$

Then, for each $k \in \mathcal{J}$, we add the waves together, so that the total wave contribution after all the Stokes lines have been crossed is

$$q_{exp} \sim \sum_{k \in \mathcal{J}} q_{exp,k}. \quad (3.27)$$

In summary, the procedure to derive the exponentially small waves for an N -cornered ship is as follows: (i) compute the first two terms of an asymptotic approximation for q and θ in (3.2) and (3.3); (ii) for each singularity of q_0 , compute χ_k in (3.8) and apply conditions (3.11) to determine whether the Stokes line intersects the free surface, i.e. determine the set \mathcal{J} in (3.16); (iii) for each $k \in \mathcal{J}$, compute the constants, c_k , γ_k , $\Omega(\sigma_k)$ from (3.12), (3.20), and (3.25); finally (iv) determine the individual waves (3.26) and sum all the contributions according to (3.27).

4. The non-existence of waveless ships

Let us see what would be needed to produce a waveless ship.

The wave contributions (3.26) are written in terms of different singulants, χ_k . To make it easier to sum them we rewrite them in terms of the single singulant, χ_1 . From (3.8), note that

$$\chi_1(w) = i \int_{-a_1}^{-a_k} \frac{d\phi}{q_0^3} + \chi_k(w), \quad (4.1)$$

where in order for the integral to exist, we may have to avoid the intermediate corners by deforming the contour into the upper half-plane. Consider now $q_{exp,k}$ in (3.26) when w is evaluated on the free surface, that is, for $w \in \mathbb{R}^+$. In the appendix of Trinh *et al.* (2011), it was shown that

$$\exp \left[-\text{Im} \left(3 \int_{-a_1}^w \frac{\mathcal{H}\theta_1}{q_0^3} d\phi \right) \right] = q_0^3(w) e. \quad (4.2)$$

Moreover, the real part of $\chi_1(w)$ comes from the residue of the integrand at $w = \infty$. We can verify that corresponding to analytic continuation into the upper half- w -plane,

$$\text{Re}(\chi_1) = 3\pi \sum_{i=1}^N a_i \sigma_i. \quad (4.3)$$

This result is derived by expanding (3.2b) as $w \rightarrow \infty$, substituting into (3.8), and integrating along a semi-circular contour.

Putting the above results together with (3.26) we find, for $w \in \mathbb{R}^+$,

$$q_{exp,k} \sim \frac{\mathcal{A}_k}{q_0^2(w)} \exp \left[-\frac{3\pi}{\epsilon} \sum_{i=1}^N a_i \sigma_i \right] \cos \left[-\frac{\text{Im}(\chi_1(w))}{\epsilon} + \text{Re} \left(3 \int_{-a_1}^w \frac{\mathcal{H}\theta_1}{q_0^3} d\phi \right) + \Psi_k \right] \tag{4.4a}$$

where the dependence on k arises only through the constants

$$\mathcal{A}_k = \frac{4\pi e |c_k|^{6-3\gamma_k} \Omega(\sigma_k)}{\epsilon^{\gamma_k} 2(1+3\sigma_k)^{\gamma_k}} \exp \left[\text{Im} \left(3 \int_{-a_1}^{-a_k} \frac{\mathcal{H}\theta_1}{q_0^3} d\phi \right) \right] \exp \left[-\frac{1}{\epsilon} \text{Im} \left(\int_{-a_1}^{-a_k} \frac{d\phi}{q_0^3} \right) \right], \tag{4.4b}$$

$$\Psi_k = \frac{1}{\epsilon} \text{Re} \left(\int_{-a_1}^{-a_k} \frac{d\phi}{q_0^3} \right) - \text{Re} \left(3 \int_{-a_1}^{-a_k} \frac{\mathcal{H}\theta_1}{q_0^3} d\phi \right) + \frac{\pi}{2} + \frac{\pi\gamma_k}{2} + (6-3\gamma_k)\theta_k. \tag{4.4c}$$

4.1. On the two-cornered ship (2-hull)

We have already shown in Trinh *et al.* (2011) that a single-cornered hull must produce waves. Therefore let us consider first the next simplest case of a 2-hull. For such a ship to be waveless, both corners must generate Stokes lines that intersect the free surface, and the waves generated by each must exactly cancel; then, there will be a finite section of free surface containing waves, but no wavetrain at infinity (as happens in the case of capillary waves in Chapman & Vanden-Broeck 2002).

In order for the waves from the two corners to cancel, we need $\mathcal{A}_1 = \mathcal{A}_2$ from (4.4b). Now for a fixed value of ϵ this may be possible (and we give such an example in § 5), but what if we want the waves to vanish for all (small) values of ϵ ? Then, since each \mathcal{A}_k is of the form

$$\lambda_1 \epsilon^{\lambda_2} e^{-\lambda_3/\epsilon}, \tag{4.5}$$

as $\epsilon \rightarrow 0$ and for real constants $\lambda_1, \lambda_2, \lambda_3$, we need the exponentials to be equal, the powers of ϵ to be equal, and the prefactors to be equal. In order for the exponentials to be equal, we see from (4.4b) that

$$\text{Im} \left(\int_{-a_1}^{-a_2} \frac{d\phi}{q_0^3} \right) = 0. \tag{4.6}$$

From (3.12) and (3.14), we have

$$\arg(1/q_0^3) = -3\theta_k \quad \text{for } w \in (-a_k, -a_{k+1}) \tag{4.7}$$

and the only way (4.6) can hold is if $\theta_1 = \pi/3$, so that q_0^3 is real for $w \in (-a_1, -a_2)$. Now, for the algebraic factors of ϵ to be equal, we require $\gamma_1 = \gamma_2$, which implies $\sigma_1 = \sigma_2$. Thus the only possibility for a waveless 2-hull is for a ship with $\sigma_1 = \sigma_2 = 1/3$. To eliminate this final possibility we need to consider the prefactors of (4.4b). Since along the real w -axis, it follows by definition of (2.13) that

$$\text{Im}(\mathcal{H}\theta_1) = \begin{cases} 0, & w < 0, \\ \theta_1(w), & w > 0, \end{cases} \tag{4.8}$$

and q_0^3 is real for $-a_1 < w < -a_2$, then

$$\text{Im} \left(3 \int_{-a_1}^{-a_2} \frac{\mathcal{H}\theta_1}{q_0^3} d\phi \right) = 0. \tag{4.9}$$

The only remaining difference between the two prefactors is in c_k (3.12). However, since

$$c_1^3 = \frac{a_1^2}{(a_1 - a_2)} \quad \text{and} \quad c_2^3 = \frac{a_2^2}{(a_1 - a_2)}, \quad (4.10)$$

the only way that we can have $|c_1| = |c_2|$ is if $a_1 = a_2$. Thus the two prefactors (4.4b) must be different, one corner always dominates the other one, and the waves can never cancel. Waveless ships with two corners are not possible.

4.2. On general N -cornered ships (N -hulls)

What can we say about more general ships? Let us take a general N -hull with the following assumptions: suppose that all the Stokes lines intersect the free surface, that $\sigma_k > 0$ for each k , and that $\theta_N \leq 2\pi/3$. In figure 1, hulls (a–e) satisfy this requirement, whereas hulls (f–h) do not. Under these assumptions, θ_k is monotonically increasing with k , so that $\arg(1/q_0^3)$ is monotonically decreasing. Thus the argument of the exponential

$$-\frac{1}{\epsilon} \operatorname{Im} \left(\int_{-a_1}^{-a_k} \frac{d\phi}{q_0^3} \right) \quad (4.11)$$

is convex in k , increasing while $0 < \theta_k < \pi/3$ and then decreasing while $\pi/3 < \theta_k < 2\pi/3$. Thus if $\theta_j \neq \pi/3$ for all j then we can see immediately that the waves generated at the corner k such that $\theta_{k-1} < \pi/3 < \theta_k$ exponentially dominate all the others. On the other hand, if $\theta_k = \pi/3$ then the waves from corners k and $k+1$ have the same exponential factor (as in the 2-hull case). If we further impose $\sigma_k = \sigma_{k+1}$ then they have the same algebraic factor, and there is possibility of wave cancellation if the prefactors are equal.

Of course, even if we could get the prefactors to be equal, we still have to worry about the waves generated by all the other corners. In fact, even from these two corners there would be higher-order correction terms (both in the form $\epsilon e^{-c/\epsilon}$, $\epsilon^2 e^{-c/\epsilon}$, etc. and also in the form of a trans-series $e^{-c/\epsilon}$, $e^{-2c/\epsilon}$ etc.). Thus it does not seem to be worth pursuing the analysis further. However, even if we cannot get the waves to cancel exactly, we might expect a significant reduction in the amplitude of the waves in the case when leading-order cancellation occurs.

4.3. On particular N -cornered ships

This brings us to the natural question of whether the analysis we have presented may be used to design a hull to minimize the wave drag. Before we address this question, let us first demonstrate that the hulls shown in figure 1(f–h) must generate waves on the free surface.

We consider them in reverse order. The 9-hull shown in figure 1(h) has $|\mathcal{J}| = 5$ (as shown in figure 3), with $\arg(1/q_0^3)$ alternating between zero and $-3\pi/2$; thus the argument above can be used to show that the contribution from $w = -a_1$ exponentially dominates all the others. The 6-hull shown in figure 1(g) has $|\mathcal{J}| = 4$, with three positive angles σ and one negative angle. Thus the algebraic factor in the contribution from $w = -a_5$ is different to the others, and those waves must always exist on the free surface.

Finally let us consider the 3-hull shown in figure 1(f), which is found in the work of Farrow & Tuck (1995), and for which the addition of a downward-pointing bulb was shown to dramatically reduce the wave resistance compared to a rectangular ship. In

this case, $|\mathcal{J}| = 1$, and $w = -a_3$ is the only relevant corner, so there are always waves on the free surface. The principal effect of the bulb is to lower the usual singularity farther away from the free surface, thereby decreasing the amplitude of the waves.

This last example not only highlights the difficulty in trying to minimize the wave drag, but also the advantage of our semi-analytic approach: we have gained considerable insight into the mechanism of wave production; from this, we can immediately see why Farrow & Tuck obtained the results that they did.

In trying to design reduced-wave hulls, it is crucial to specify what exactly is the optimization process. For example, if we simplify the hull of Farrow & Tuck to a 2-hull by reducing the width of the downward-pointing bulb to zero, then we have one parameter, a_1 , over which we can optimize (since $a_1 + a_2 = 1$). We find the smallest waves occur for $a_1 = 0.5$, i.e. when there is no bulb. However, in our current non-dimensionalization, as we vary a_1 , both the depth of the hull and that of the bulb vary. If instead we fix the depth of the hull, and allow the depth of the bulb to vary, we find that the waves get smaller as the bulb gets deeper. On the other hand, if we fix the depth of the bulb, and allow the depth of the hull to vary, we again find that the smallest waves correspond to the hull depth being equal to the bulb depth, i.e. to there being no bulb.

5. Numerical and asymptotic results for two-cornered hulls

The numerical algorithms developed in Trinh *et al.* (2011) can be used to verify the asymptotic predictions. Here, we focus on the particular case of a 2-hull, which we refer to as a $[\sigma_1, \sigma_2]$ -hull; this is a ship with divergent corner angles σ_1 and σ_2 , and with leading-order flow given by (2.9), or

$$q_s = \frac{w^{\sigma_1 + \sigma_2}}{(w + a_1)^{\sigma_1} (w + a_2)^{\sigma_2}}, \quad (5.1)$$

with $a_1 + a_2 = 1$.

As we discussed in Trinh *et al.* (2011), the numerical computation of the stern problem at small values of ϵ can be particularly difficult, and the culprit is the presence of the attachment singularity at $w = 0$ associated with a small boundary layer; this singularity is responsible for most of the numerical error. For hulls where the in-fluid attachment angle between the free surface and body is less than $\pi/3$, a simple finite-difference scheme based on the methods outlined in Vanden-Broeck & Tuck (1977) can be used, provided that we limit our search to waves larger than $\approx 10^{-4}$. Figure 4 provides an example of solutions found using this method.

The theory of §§ 3 and 4 can be verified by comparing the analytical predictions with numerically computed wave amplitudes far from the ship. First, consider the effect of varying the Froude number on ships of a fixed geometry. This is shown in figure 5 for three 2-hulls with their corners fixed with $a_1 = 0.8$ and $a_2 = 0.2$. The individual cosine waves are calculated from (3.26) with $q_0 \rightarrow 1$ downstream, and then the final amplitude computed using the sum (3.27) (see § 4.5 in Trinh 2010*b* for additional details). The match between numerical and asymptotic solutions is quite good, and like the previous work, we remark that the results are applicable over a wide range of Froude numbers.

Next, we would like to consider the effect of fixing the Froude number, but varying the positions of the corners. The problem, however, is that the interesting effects of this procedure are only seen at values of ϵ much smaller than those we can achieve

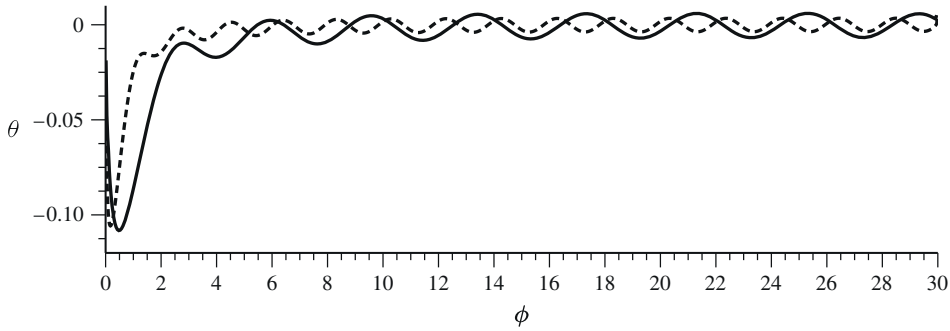


FIGURE 4. Solutions for the [0.5, 0.125]-hull (dashed line) and [0.25, 0.25]-hull (solid line) at $\epsilon = 2/3$ and $\epsilon = 1/3$, respectively. Both ships have corners set at $a_1 = 0.8$ and $a_2 = 0.2$. The solutions were computed using ALGORITHM A of Trinh *et al.* (2011) with the number of mesh points, $n = 1000$ and grid spacing, $\Delta\phi = 0.015$ for the former ship and $n = 2000$ and $\Delta\phi = 0.015$ for the latter.

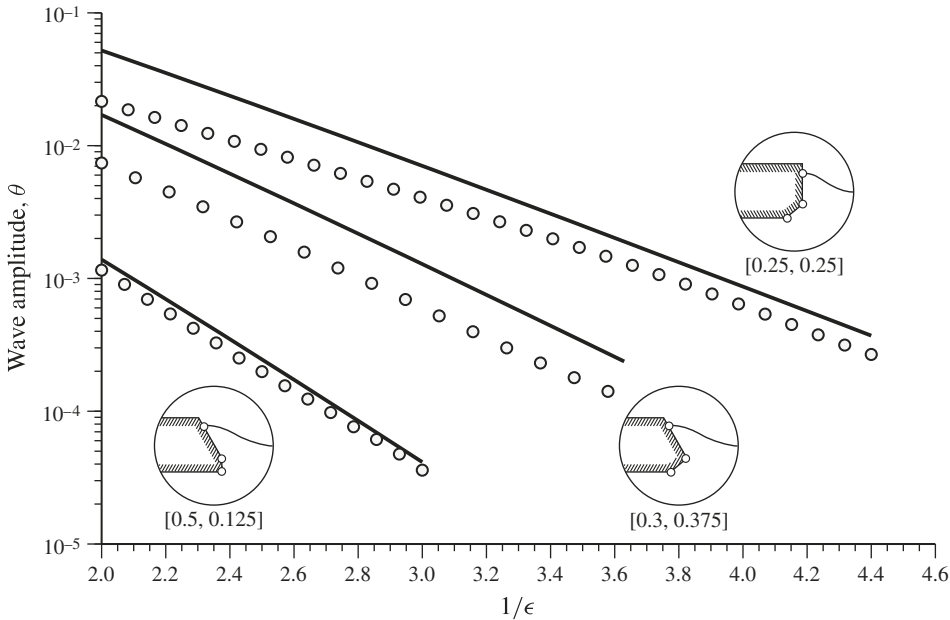


FIGURE 5. Numerical (circles) and asymptotic (solid) amplitudes of the downstream waves for a range of hull inclinations. In all cases, the corner points are fixed with $a_1 = 0.8$ and $a_2 = 0.2$. The solutions were computed using ALGORITHM A of Trinh *et al.* (2011). The parameters used were the following: $n = 1000$, $\Delta\phi = 0.04$ (bottom); $n = 1500$, $\Delta\phi = 0.03$ (middle); and $n = 2000$, $\Delta\phi = 0.025$ (top).

using the above numerical methods. In the [Appendix](#), we present a slightly simplified version of the ship-wave problem (2.12a)–(2.12b) that preserves the asymptotic structure of the waves, but also enables us to compute numerical solutions to much higher accuracy.

This simplified problem was used to create figure 6, which shows the effect of varying the positions of the corners on the wave amplitude for a [1/4, 1/4]-hull

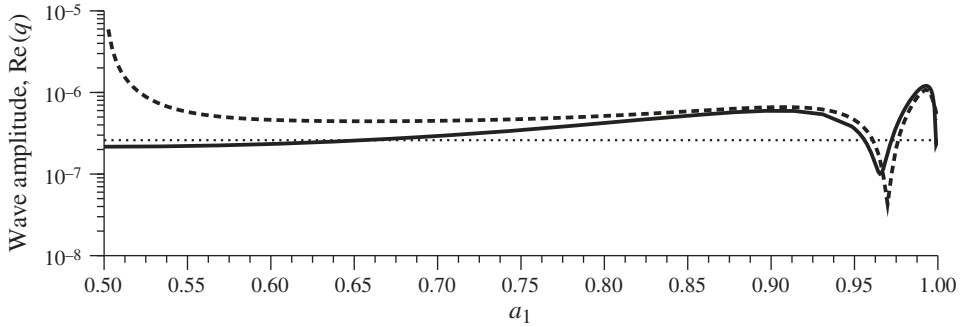


FIGURE 6. The numerical solution (solid) is plotted against the asymptotic approximation (dashed) for the simplified nonlinear problem of the [Appendix](#). The ship is a $[1/4, 1/4]$ -hull with $a_1 + a_2 = 1$ and $\epsilon = 0.15$. The dotted line indicates the one-cornered approximation for a rectangular hull.

with $\epsilon = 0.15$, $a_1 + a_2 = 1$, and values of $0.5 \leq a_1 \leq 1$. The figure contains a number of interesting effects: the first is that the numerically computed wave amplitude shows a significant dip (an order of magnitude) near $a_1 \approx 0.96$, and that this effect is also captured fairly accurately in the asymptotic solution.

The reason for the dip is that, near $a_1 \approx 0.96$, the waves from the two corners exhibit partial destructive interference. However, from the previous section, we know that the waves generated by the corner at $-a_2$ should exponentially dominate those from $-a_1$. How then are they cancelling each other? The answer is that the prefactor $|c_1|^{6-3\gamma_1}$ is over ten times larger than $|c_2|^{6-3\gamma_1}$; at this particular value of ϵ , the difference in prefactors is enough to compensate for the difference in exponentials, since

$$\text{Im} \left(\int_{-a_1}^{-a_2} \frac{d\phi}{q_0^3} \right) \quad (5.2)$$

is not particularly large. Thus, the value of a_1 at which cancellation occurs depends on ϵ ; for somewhat smaller values of ϵ the Stokes line from $w = -a_2$ does indeed dominate and no cancellation is possible. This indicates that it should be possible to design hulls with reduced wave drag at a particular speed (Froude number). It is also reassuring to note that including the leading-order term from each of our exponentially small waves captures the behaviour of the solution very well, even though, formally, one of the terms is exponentially subdominant.

The second effect illustrated by figure 6 is the divergence between our asymptotic expansion and the numerical solution for values of a_1 close to 0.5. The reason for the divergence is that the prefactors c_1 and c_2 are singular as the corners approach each other; our analysis in § 3, in fact, implicitly assumes that the corners of the ship are spaced sufficiently far from one another.

To be more specific, in order to determine the constants γ_k and Λ_k in (3.20) and (3.21) in the previous analysis, the outer solution was required to match a nonlinear inner solution. The size of this inner region can be derived by observing where the breakdown in the outer expansion (3.1) first occurs, i.e. where $\epsilon q_1 \sim q_0$. From (3.2b) and (3.3b), the required re-scaling of w near a singularity at $-a_k$ can be seen to be

$$w + a_k = O(\epsilon^{1/(1+3\sigma)}). \quad (5.3)$$

Thus, if two (or more) singularities are spaced within a distance of (5.3) apart, then the previous asymptotic methodology breaks down as $\epsilon \rightarrow 0$. If we combine the two corners into a single corner of angle $\pi/2$, we find the wave amplitude given by the dotted line in figure 6. This approximation clearly works well for a_1 close to 0.5.

A uniform approximation would need to smoothly match with the one-cornered approximation at one end, and the (separated) two-cornered analysis at the other, and thus bridges the dashed and dotted lines in figure 6. Such an approximation requires us to consider the distinguished limit in which the corners of the ship are allowed to approach one another as $\epsilon \rightarrow 0$. This is similar to the situation in Chapman & Vanden-Broeck (2006, Appendix B) where the asymptotic solutions for flow over a rectangular step in a channel were analysed in the case where both corners of the step lie in the same ‘inner region’. For the case of the multi-cornered ship, the details of this analysis are very technical, and will be published in a future paper.

6. Discussion

In the end, what is the definitive answer to the conundrum of existence and non-existence of waveless ships? Unlike our results for the single-cornered ships of Trinh *et al.* (2011), there does not seem to be a simple answer to this question, applicable to the most general piecewise-linear hulls. Despite this, however, we have offered several new insights into the study of ship-wave resistance: we have offered explicit formulae for the computation of waves given the shape of the ship’s hull; we have offered simple interpretations of the production of such waves in terms of Stokes-line crossings and the Stokes phenomenon; and perhaps most importantly, we offered a methodology which, given specific ships, provides an immediate and intuitive understanding of the effect of the body on the free surface.

In the previous work, we highlighted the importance of distinguishing between local and global properties of the analysis. Consider the factorial-over-power divergence of the asymptotic series in (3.4), or the emergence conditions of Stokes lines in (3.15), or the numerically determined prefactor, Ω_k , in (3.25) – these are all local properties of the problem; indeed their derivation only depends on the behaviour of the asymptotic solution near the relevant singularities. These local properties, we understand well.

In contrast, many global questions remain unanswered. For example, given a ship, represented by q_0 , what are the necessary and sufficient conditions for Stokes lines to intersect the free surface? In §3.2, we assumed that only Stokes lines that emerge on the same Riemann sheet are relevant. Is this always the case? (See, *e.g.* Chapman & Mortimer (2005), Chapman, Trinh & Witelski (2013), Trinh & Chapman (2013*b*) for scenarios where this may not be true.) Or perhaps more difficult: what are the necessary restrictions on q_0 so that total phase cancellation occurs? We have provided a few preliminary results on this global problem, but a more exhaustive analysis of these issues remains an open problem.

Naturally, our study of ship waves would be incomplete without a theory applicable for smooth hulls, with the eventual goal of addressing the well-known technique of using a bulb to reduce the wave resistance of a ship (Baba 1976). However, the difficulty here is that analytic continuation is an ill-posed process and small perturbations in the shape of a hull can have large effects on the associated singularities – a unified theory for arbitrary ship geometries is likely to prove difficult, if not downright impossible.

Perhaps, then, we should only consider specific classes of smooth ships. Ship waves associated with continuous geometries have been considered in the numerical work

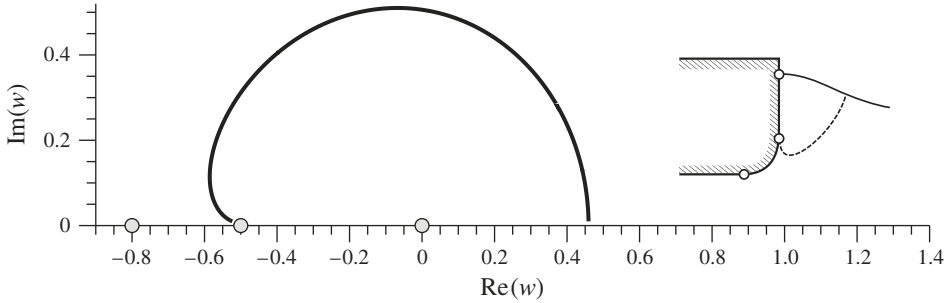


FIGURE 7. Stokes lines for the smoothed hull in (6.2) with $a_1 = 0.8$ and $a_2 = 0.5$. The Stokes line leaves tangentially along the boundary, but later intersects the free surface.

of Tuck & Vanden-Broeck (1984), Madurasinghe (1988), and Farrow & Tuck (1995), where there, the hulls are specified by piecewise-entire functions. For example, Farrow & Tuck (1995) consider the family of hulls given by

$$\theta = \begin{cases} 0 & \text{for } w \in (-\infty, -1) \\ A(w + 1)(w + b) + \frac{\pi}{2} \frac{(w + 1)}{(1 - b)} & \text{for } w \in (-1, -b) \\ \frac{\pi}{2} & \text{for } w \in (-b, 0), \end{cases} \quad (6.1)$$

which, given parameters A and b , provides a ship consisting of a horizontal bottom and a vertical line, joined by a rounded section; $A > 0$ yields rounded corners and $A < 0$ yields bulbous sterns. The key is that if we restrict ourselves to classes of ships given by piecewise-entire functions, then the complex singularities must be located at the points joining each piece. As a simpler example, we may consider the ship with

$$\theta = \begin{cases} 0 & \text{for } w \in (-\infty, -a_1) \\ \frac{\pi}{2} \left[1 + \frac{(w + a_2)}{(a_1 - a_2)} \right] & \text{for } w \in (-a_1, -a_2) \\ \frac{\pi}{2} & \text{for } w \in (-a_2, 0), \end{cases} \quad (6.2)$$

which is similar to the vertically faced one-cornered ships studied previously, but with a rounded edge. Analysis of the Stokes lines shows that the relevant line emerges from $w = -a_2$; this is shown in figure 7. The study of these piecewise-entire ships is the subject of ongoing investigation.

A similar direction for research is towards the development of a low-Froude-number asymptotic theory for flows past three-dimensional, full-bodied ships. This builds upon the works of, for example, Keller (1979) and Brandsma & Hermans (1985), who apply geometrical ray theory to the case of streamline (thin) ships. In theory, the interpretation we have presented in this paper of free-surface waves arising from Stokes-line crossings is still valid in three dimensions, except now singularities are associated with Stokes surfaces rather than lines. In practice, however, the analysis is complicated due to the loss of complex-variable techniques. We refer the reader to the work of Chapman & Mortimer (2005), which provides a first step towards extensions of exponential asymptotics to partial differential equations.

In addition to our study, which solely focuses on the low-Froude-number model of Dagan & Tulin (1972), it is important for us to question the place of these simplified

mathematical models in terms of the bigger picture: that which includes the effects of vorticity, viscosity, and time-dependence in ship-wave interactions. As we elucidated in the introduction, numerical work (as particular examples, see Grosenbaugh & Yeung 1989 and Yeung & Ananthkrishnan 1997) show that in practice, these neglected effects can have significant roles in the production of waves. Extended discussions of the role of low-Froude-number theories appear in Tuck & Vanden-Broeck (1984, p. 301), Tuck (1991a), and Tulin (2005). Thus, while it is certainly true that in order to obtain analytical approximations directly relating ship geometries to free-surface waves, the low-Froude-number approximation provides enormous simplification, we hope that similar analytical theories can be developed which include a more complete host of effects.

Appendix. The simplified nonlinear problem

The full problem in (2.12a)–(2.12b) can be studied using the methods we develop here, but can also work with a simpler problem that nevertheless contains all of the the key components. The reason for this simplification is that, in order to verify the asymptotic analysis in the regime where the ship’s corners are closely spaced, wave amplitudes must be computed to five or six digits of precision – otherwise, the fine effects of adjusting the ship’s geometry are easily missed; this precision can only be easily achieved for the simpler problem, which we now derive.

As we know, when exponentially small terms are sought from (2.12a), the integral term, $\mathcal{H}\theta$, only plays a minor role throughout the analysis. If we return to the derivation of the late-orders ansatz (3.4), we recall that the subdominance of $\mathcal{H}\theta$ as $n \rightarrow \infty$ ensures that it plays no part in the derivation of χ_k . In fact, the only role of the Hilbert transform is to change the expression for q_1 in (3.3b). Consequently, in the final form of the waves $q_{exp,k}$ in (3.26), the presence of $\mathcal{H}\theta_1$ only serves to change the amplitude coefficient and the phase shift by an $O(1)$ amount.

Therefore, the salient features of the problem can still be retained if we use $\log q \pm i\theta = \log q_s$ instead of (2.12a); this way, we simplify the full problem in (2.12a)–(2.12b) to a single nonlinear differential equation in q . Analytic continuation into the upper half-plane, and substituting $i\theta = \log(q_s/q)$ into (2.12b) gives

$$\epsilon q_s q^3 \frac{dq}{dw} + \frac{i}{2} [q^2 - q_s^2] = 0, \quad (\text{A } 1)$$

which can be solved subject to the single boundary condition $q(0) = 0$. It is more convenient to work under the substitution $u(w) = q^2(w)$, where we have

$$\epsilon q_s u \frac{du}{dw} + i[u - q_s^2] = 0, \quad (\text{A } 2)$$

as a simplified nonlinear model of ship waves. Simplifications of the boundary-integral problem (2.12a) and (2.12b) were also proposed in Tuck (1991a,b), but there, the simplifications were argued based on behavioural requirements. Here, (A 1) is a justified reduction based on the $\epsilon \rightarrow 0$ limit.

Notice that in this new problem, we chose to analytically continue into the upper half- w -plane, and thus the exponentially small waves of (A 1) will possess both a real and imaginary part. If we wish, we can mirror the analysis for the lower half- w -plane and add the complex conjugate as we did before for (3.19).

However, it is somewhat simpler to examine (A 1) as a problem on its own; thus we shall only concern ourselves with studying the real component of the solution to (A 1),

which we write $\bar{q}_{\text{exp}} = \text{Re}(q_{\text{exp}})$. Now instead of (3.26), the form of the waves for the simplified problem (with well-separated corners) is given by

$$\begin{aligned} \bar{q}_{\text{exp},k} \sim & \frac{2\pi}{\epsilon^{\gamma_k}} \frac{|c_k|^{6-3\gamma_k}}{2(1+3\sigma_k)^{\gamma_k}} \frac{\Omega(\sigma_k)}{q_0^5} \exp\left[-\frac{\text{Re}(\chi_k)}{\epsilon}\right] \\ & \times \cos\left[-\frac{\text{Im}(\chi_k)}{\epsilon} + \frac{\pi\gamma_k}{2} + (6-3\gamma_k)\theta_k\right], \end{aligned} \quad (\text{A } 3)$$

which is effectively (3.26) with $\mathcal{H} \equiv 0$ and without a phase shift of $\pi/2$. The reduction by a factor of 2 in (A 3) compared to (3.26) occurs because there is no need to add the complex-conjugate wave contribution. Analytical and numerical results for the simplified nonlinear problem of (A 1) in the context of a one-cornered ship can be found in Trinh *et al.* (2011), whereas we have already discussed the numerical solution of the [1/4, 1/4]-hull for the simplified problem in § 5 and figure 6.

REFERENCES

- BABA, E. 1976 Wave breaking resistance of ships. In *Proceedings of International Seminar on Wave Resistance*, pp. 75–92. Tokyo.
- BOYD, J. P. 1998 *Weakly Non-local Solitary Waves and Beyond-all-orders Asymptotics*. Kluwer.
- BRANDSMA, F. J. & HERMANS, A. J. 1985 A quasi-linear free surface condition in slow ship theory. *Schiffstechnik Bd.* **32**, 25–41.
- CHAPMAN, S. J., KING, J. R. & ADAMS, K. L. 1998 Exponential asymptotics and Stokes lines in nonlinear ordinary differential equations. *Proc. R. Soc. Lond. A* **454**, 2733–2755.
- CHAPMAN, S. J. & MORTIMER, D. B. 2005 Exponential asymptotics and Stokes lines in a partial differential equation. *Proc. R. Soc. Lond. A* **461**, 2385–2421.
- CHAPMAN, S. J., TRINH, P. H. & WITELSKI, T. P. 2013 Exponential asymptotics for thin film rupture. *SIAM J. Appl. Maths* **73** (1), 232–253.
- CHAPMAN, S. J. & VANDEN-BROECK, J.-M. 2002 Exponential asymptotics and capillary waves. *SIAM J. Appl. Maths* **62** (6), 1872–1898.
- CHAPMAN, S. J. & VANDEN-BROECK, J.-M. 2006 Exponential asymptotics and gravity waves. *J. Fluid Mech.* **567**, 299–326.
- DAGAN, G. & TULIN, M. P. 1969 Bow waves before blunt ships. *Tech. Rep.*, Office of Naval Research, Department of the Navy.
- DAGAN, G. & TULIN, M. P. 1972 Two-dimensional free-surface gravity flow past blunt bodies. *J. Fluid Mech.* **51** (3), 529–543.
- DINGLE, R. B. 1973 *Asymptotic Expansions: Their Derivation and Interpretation*. Academic.
- FARROW, D. E. & TUCK, E. O. 1995 Further studies of stern wavemaking. *J. Austral. Math. Soc. B* **36**, 424–437.
- GROSENBAUGH, M. A. & YEUNG, R. W. 1989 Nonlinear free-surface flow at a two-dimensional bow. *J. Fluid Mech.* **209**, 57–75.
- HOCKING, G. C., HOLMES, R. J. & FORBES, L. K. 2012 A note on waveless subcritical flow past a submerged semi-ellipse. *J. Eng. Math.* **81** (1), 1–8.
- KELLER, J. B. 1979 The ray theory of ship waves and the class of streamlined ships. *J. Fluid Mech.* **91**, 465–487.
- KOSTYUKOV, A. A. 1968 *Theory of Ship Waves and Wave Resistance*. Effective Communications.
- KOTIK, J. & NEWMAN, D. J. 1964 A sequence of submerged dipole distributions whose wave resistance tends to zero. *J. Math. Mech.* **13**, 693–700.
- KUZNETSOV, N., MAZ'YA, V. & VAINBERG, B. 2002 *Linear Water Waves: A Mathematical Approach*. Cambridge University Press.
- LUSTRI, C. J., MCCUE, S. W. & BINDER, B. J. 2012 Free surface flow past topography: a beyond-all-orders approach. *Eur. J. Appl. Maths* **1** (1), 1–27.

- MADURASINGHE, M. A. D. 1988 Splashless ship bows with stagnant attachment. *J. Ship Res.* **32** (3), 194–202.
- MADURASINGHE, M. A. D. & TUCK, E. O. 1986 Ship bows with continuous and splashless flow attachment. *J. Austral. Math. Soc. B* **27**, 442–452.
- NEWMAN, J. N., WEBSTER, W. C., WU, G. X., MYNETT, A. E., FAULKNER, D. & VICTORY, G. 1991 The quest for a three-dimensional theory of ship-wave interactions [and discussion]. *Phil. Trans. R. Soc. Lond. A* **334** (1634), 213–227.
- OGILVIE, T. F. 1968 Wave resistance: The low speed limit. *Tech. Rep.*, Michigan University, Ann Arbor.
- OGILVIE, T. F. 1970 Singular perturbation problems in ship hydrodynamics. *Tech. Rep.*, Michigan University, Ann Arbor.
- OLDE DAALHUIS, A. B., CHAPMAN, S. J., KING, J. R., OCKENDON, J. R. & TEW, R. H. 1995 Stokes Phenomenon and matched asymptotic expansions. *SIAM J. Appl. Maths* **55** (6), 1469–1483.
- PAGANI, C. D. & PIEROTTI, D. 2004 The subcritical motion of a semisubmerged body: solvability of the free boundary problem. *SIAM J. Math. Anal.* **36** (1), 69–93.
- STOKER, J. J. 1957 *Water Waves: The Mathematical Theory with Applications*. Interscience Publishers, Inc.
- TRINH, P. H. 2010a Exponential asymptotics and Stokes line smoothing for generalized solitary waves. In *Asymptotic Methods in Fluid Mechanics: Survey and Recent Advances* (ed. Steinrück Herbert), pp. 121–126. Springer.
- TRINH, P. H. 2010b Exponential asymptotics and free-surface flows. PhD thesis, University of Oxford.
- TRINH, P. H. & CHAPMAN, S. J. 2013a New gravity-capillary waves at low speeds. Part 1. Linear theory. *J. Fluid Mech.* **724**, 367–391.
- TRINH, P. H. & CHAPMAN, S. J. 2013b New gravity-capillary waves at low speeds. Part 2. Nonlinear theory. *J. Fluid Mech.* **724**, 392–424.
- TRINH, P. H., CHAPMAN, S. J. & VANDEN-BROECK, J.-M. 2011 Do waveless ships exist? Results for single-cornered hulls. *J. Fluid Mech.* **685**, 413–439.
- TUCK, E. O. 1991a Ship-hydrodynamic free-surface problems without waves. *J. Ship Res.* **35** (4), 277–287.
- TUCK, E. O. 1991b Waveless solutions of wave equations. In *Proceedings 6th International Workshop on Water Waves and Floating Bodies*. MIT.
- TUCK, E. O. & VANDEN-BROECK, J.-M. 1984 Splashless bow flows in two-dimensions. In *Proceedings of 15th Symp. Naval Hydrodynamics*. National Academy.
- TULIN, M. P. 2005 Reminiscences and reflections: Ship waves, 1950–2000. *J. Ship Res.* **49** (4), 238–246.
- VANDEN-BROECK, J.-M., SCHWARTZ, L. W. & TUCK, E. O. 1978 Divergent low-Froude-number series expansion of nonlinear free-surface flow problems. *Proc. R. Soc. Lond. A* **361**, 207–224.
- VANDEN-BROECK, J.-M. & TUCK, E. O. 1977 Computation of near-bow or stern flows using series expansion in the Froude number. In *2nd International Conference on Numerical Ship Hydrodynamics*. Berkeley, California: University of California, Berkeley.
- YEUNG, R. W. & ANANTHAKRISHNAN, P. 1997 Viscosity and surface-tension effects on wave generation by a translating body. *J. Engng Maths* **32** (2), 257–280.